ACS Catalysis

pubs.acs.org/acscatalysis Research Article

Water-Controlled Coking Dynamics during High-Pressure Methanol-to-Olefins Reaction over SAPO-34

Chengwei Zhang, Xinqiang Wu,* Yanan Zhang, Li Wang, Yan Jin, Mingbin Gao, Mao Ye, Yingxu Wei,* and Zhongmin Liu

Cite This: *ACS Catal.* 2025, 15, 1553−1562 Read Online

ACCESS | Metrics & More | Article Recommendations | Supporting Information

ABSTRACT: Water, as a co-feed and decoking agent for catalyst regeneration, is increasingly recognized as a crucial component in methanol to olefins (MTO) catalysis over zeolites. In this study, water-controlled coking dynamics and improved diffusion efficiency have been revealed in a high-pressure MTO reaction over the SAPO-34 zeolite catalyst. Through gas chromatograph−mass spectrometry (GC-MS), matrix-assisted laser desorption/ionization Fourier-transform ion cyclotron resonance mass spectrometry (MALDI FT-ICR MS), and ultraviolet−visible spectroscopy (UV−vis), the kinetic behavior of water-delayed coking has been confirmed mainly in two aspects: suppressing the aging of active hydrocarbon pool species (HCPs, e.g., phenyl, naphthyl species) to form polyaromatic hydrocarbons (PAHs) within the CHA cages and hindering the cross-linking of PAHs between CHA cages. For the deactivated SAPO-34 catalyst, the restoration of methanol conversion from 5% to 40% upon switching from methanol to water−methanol co-feed and from 5% to 100% after high-pressure steam treatment further confirms the in situ coke decomposition capability of high-pressure water under the real MTO reaction conditions. Moreover, structured illumination microscopy (SIM) offers a direct visualization of the retained organic species and their spatiotemporal distribution within individual SAPO-34 crystals under the influence of water, thereby providing visual evidence for water-delayed coking dynamics and the improved diffusion process. Thus, the mechanistic insights into water-controlled coking and diffusion dynamics unveiled in this study provide a crucial theoretical foundation for the application of water-related techniques in the MTO industry.

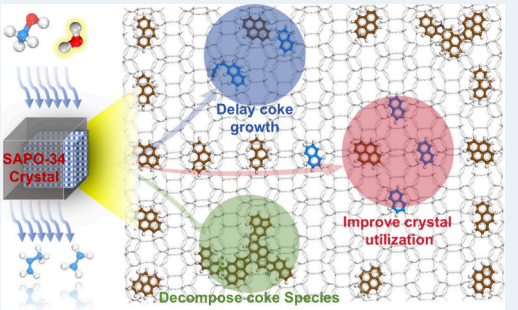

Cofeeding high-pressure water control coke dynamics

KEYWORDS: *SAPO-34, Water co-feeding, Methanol-to-olefins, Water-delayed coking and promoted diffusion dynamics*

INTRODUCTION

Water, an essential material for the survival of life on earth, plays a crucial role in the physical, chemical, and biochemical processes of nature.[1−3] With technology advancement, water has been widely applied in materials science and engineering. Zeolites, as a significant class of microporous materials, are extensively utilized in adsorption and separation, ion exchange, and catalysis due to their acidity and shape selectivity.[4−6] In catalytic applications, water influences the entire lifecycle of zeolite catalysts—from hydrothermal synthesis[7−9] and post-synthetic modification[10−12] to catalytic reaction[13,14]—by being involved in the host−guest interactions between zeolites and water and participating in catalytic reaction kinetics. This, in turn, affects the zeolite topology, acidity, and catalytic performance. Therefore, a comprehensive understanding of the host−guest interactions between zeolites and water, especially elucidating water-mediated catalytic reaction kinetics and water-induced structural dynamics of zeolites under working conditions, is crucial for advancing zeolite chemistry and catalysis science.

The methanol-to-hydrocarbons (MTH) reaction, catalyzed by zeolite materials, provides a novel route for producing light olefins and aromatics from nonpetroleum feedstocks.[15−18] SAPO-34 molecular sieve, a representative zeolite catalyst, has been widely studied and successfully applied for the methanol to olefins (MTO) industrial process.[16,19,20] Water is ubiquitous in MTO catalysis as a stoichiometric byproduct, co-feedstock, and even a regeneration agent for deactivated catalyst. The host−guest interactions between SAPO-34 and water and the influence on the MTO catalytic performance have been noted. Froment and Anthony reported that water can affect the product distribution, methanol conversion efficiency, and coke formation during MTO reaction over SAPO-34.[21,22] Ruiz-Martínez et al. found that co-feeding water could prolong catalytic lifetime, attributing this to the occupation of acidic sites by water.[23] They further discussed the role of water in different reaction stages of MTO catalysis, focusing on

Received: October 10, 2024
Revised: December 16, 2024
Accepted: January 6, 2025
Published: January 13, 2025

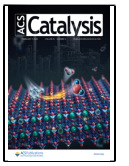

https://doi.org/10.1021/acscatal.4c06239
ACS Catal. 2025, 15, 1553−1562

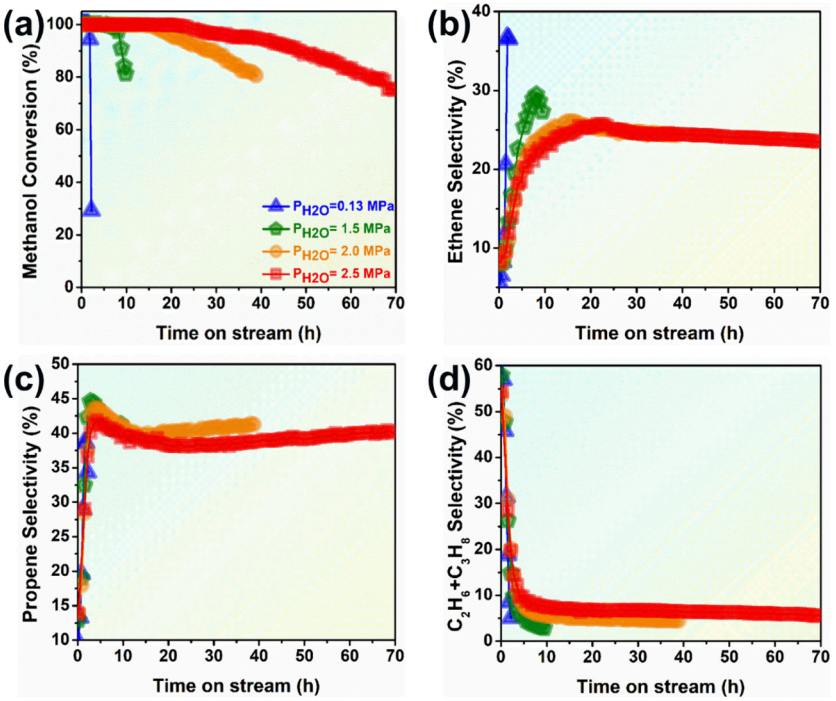

Figure 1. Catalytic performance of methanol conversion and product selectivity under the condition of co-feeding high-pressure water on SAPO-34 zeolite catalyst: (a) methanol conversion, (b) ethene selectivity, (c) propene selectivity, (d) ethane plus propane selectivity. Reaction conditions: 723 K, P_{total} = 4.0 MPa, P_{MeOH} = 0.13 MPa, methanol WHSV = 1.0 h^{-1}.

competitive adsorption with methanol and olefins at Brønsted acid sites (BASs). In our study, the deactivated SAPO-34 catalyst can be effectively regenerated through steam treatment under high temperature, a method with great potential in MTO industrial processes.[24−26] Spectroscopic evidence suggested that co-feeding water promotes the formation and retention of naphthyl species within the CHA cages of SAPO-34, and DFT calculations further confirm the role of water in proton transfer and transition state stabilization, which are crucial for selective light olefin production, especially ethene.[27] In our recent study, a superlong catalytic lifetime in high-pressure MTO reactions was achieved by co-feeding water and hydrogen, demonstrating significant synergistic effects.[28] Compared with atmospheric pressure, the high-pressure water co-feeding is more conducive to the extension of catalytic lifetime. Therefore, the impact of high-pressure water co-feeding on MTO catalytic performance and the underlying mechanisms remain unclear, necessitating further investigation. Additionally, the application of steam-assisted deactivated catalyst regeneration in the MTO industry requires a fundamental understanding of water-controlled coking dynamics and diffusion behaviors.

In this study, water-delayed coking by inhibiting the ring-fusing of aromatics within the CHA cages and cross-linking of polyaromatic hydrocarbons (PAHs) between CHA cages has been revealed by GC-MS, MALDI FT-ICR MS, and UV−vis spectroscopy during high-pressure MTO reaction on SAPO-34 zeolite catalyst. Furthermore, for the deactivated SAPO-34 catalyst, both the partial recovery of catalytic performance (methanol conversion increasing from 5% to 40%) after switching methanol to water−methanol co-feed and the significant recovery (methanol conversion rising from 5% to 100%) after high-pressure steam treatment have validated the in situ coke decomposition capability of high-pressure water under real MTO reaction conditions. Further, the enhancement of BAS utilization efficiency within the SAPO-34 catalyst was revealed by Fourier transform infrared (FTIR) spectroscopy, and the structured illumination microscopy (SIM) visualizations of the individual SAPO-34 crystals demonstrated a more uniform coke distribution and enhanced crystal utilization efficiency. These improvements in crystal utilization are attributed to the reduction in diffusion limitations of reactant molecules within the SAPO-34 micropores, resulting from the depressed growth of coke species facilitated by water. Therefore, our findings elucidate the pivotal role of water in controlling coke growth and distribution over the SAPO-34 catalyst in high-pressure MTO reaction, providing spectroscopic evidence for the water-delayed coking dynamics and promoted diffusion process. The profound insights into the role of water establish a theoretical foundation for further promoting the reaction with implementation of the strategy by co-feeding water to delay coke deposition and steam assistance for deactivated catalyst regeneration in the MTO industry.

RESULTS AND DISCUSSION

Water-Delayed Coking in High-Pressure MTO Reaction. Under atmospheric pressure MTO reaction, co-feeding water has been confirmed as an unobvious impact on the catalytic lifetime of SAPO-34 in previous studies.[21,22] However, the simultaneous co-feeding of water and hydrogen demonstrated a synergistic effect in delaying coking, thus leading to an order of magnitude increase in catalytic lifetime in high-pressure MTO reaction on SAPO-34 zeolites.[28] According to Bhan et al., even methanol−hydrogen co-feeding alone can also exhibit excellent catalytic lifetime extension.[29] Therefore, to elucidate the potential role of water in the high-pressure MTO reaction on SAPO-34 (the characterizations are shown in Figure S1), we initially investigated the impact of

https://doi.org/10.1021/acscatal.4c06239
ACS Catal. 2025, 15, 1553−1562

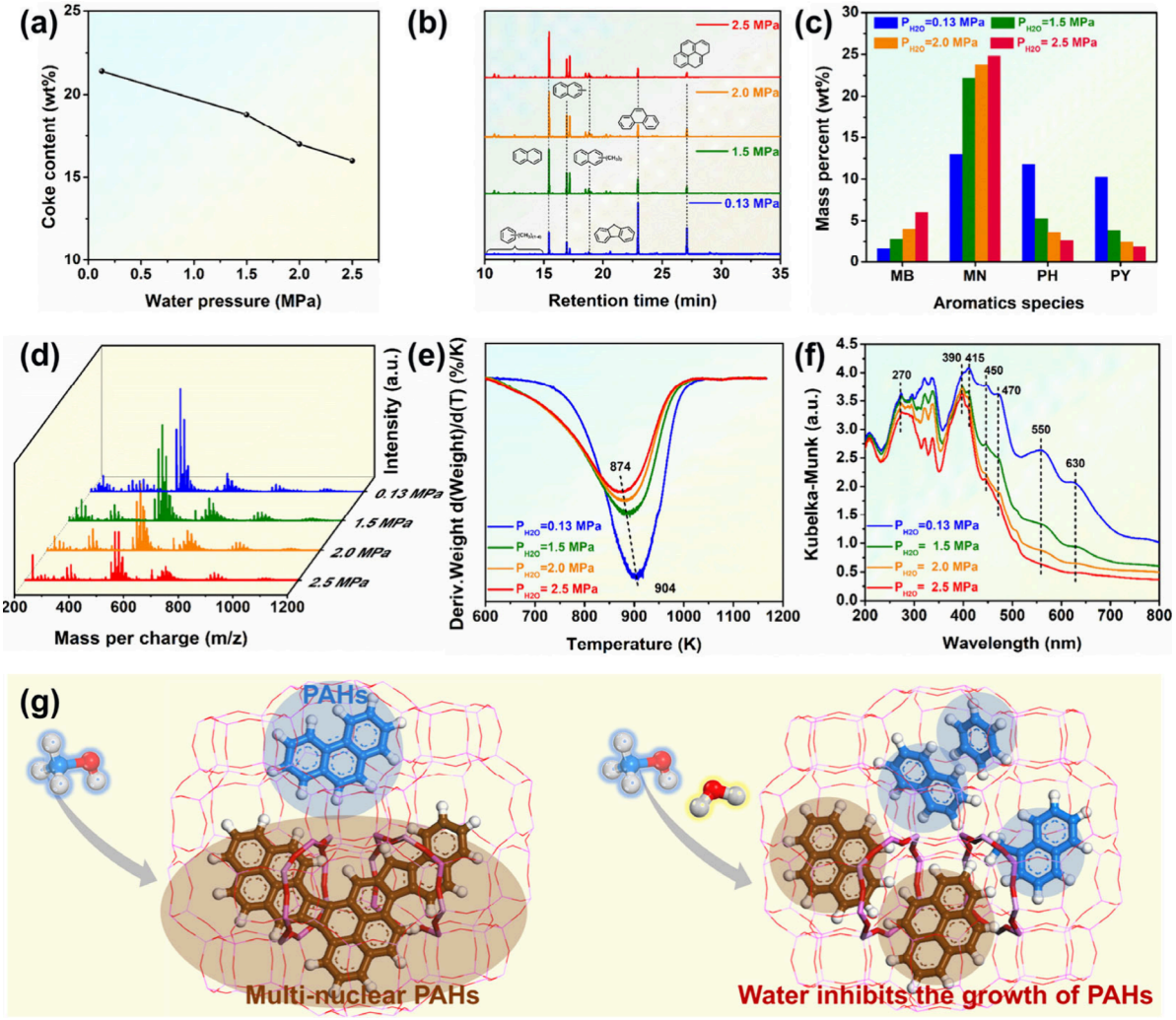

Figure 2. Effect of high-pressure water on the formation of coke over the SAPO-34 catalyst after 2 h of methanol conversion with different water partial pressures. (a) Coke content. (b) Chromatograms of CCl_4-soluble fractions of the retained organics extracted. (c) Detailed distribution of CCl_4-soluble fractions (methylbenzene (MB), methyl naphthalene (MN), phenanthrene (PH), pyrene (PY)) of the retained organics extracted among total coke. (d) The multinuclear PAHs detected by MALDI FT-ICR MS. (e) Differential thermogravimetry (DTG) profiles. (f) UV−vis spectra. (g) The molecular model of water-controlled coke growth under the high-pressure MTO reaction. Reaction conditions: 723 K, P_{total} = 4.0 MPa, P_{MeOH} = 0.13 MPa, methanol WHSV = 1.0 h^{-1}.

water−methanol co-feed on the MTO performance at 723 K, with water partial pressure ranging from 0.13 to 2.5 MPa at the total pressure of 4 MPa (Figure 1). Considering the stoichiometric water generation during methanol conversion on zeolite catalysts, the partial pressure of water in this study refers to the combined pressure of both the reaction-generated water and the added co-feed water. Figures 1(a) and S2 illustrate the MTO product selectivity and catalytic lifespan of SAPO-34 under different water partial pressures. At a low water partial pressure of 0.13 MPa, SAPO-34 rapidly deactivated, with the methanol conversion dropping to around 20% within 2 h. Generally, under the high-pressure MTO reaction conditions, a relatively long contact time between methanol/initial hydrocarbon products and SAPO-34 catalyst exacerbated the secondary reaction (e.g., hydrogen transfer, aromatization) and led to a rapid accumulation of PAHs on SAPO-34 catalyst, causing the pore blockage and coverage of acidic sites and a fast deactivation of catalyst.[30−32] However, when water was introduced as a co-fed material, the MTO catalytic lifetime of SAPO-34 catalyst significantly increased from 2 h to 70 h with the increase of water partial pressure from 0.13 MPa to 2.5 MPa. In this high-pressure water co-feeding MTO reaction, the observed enhancement of MTO catalytic lifetime is positively correlated with the water partial pressure. In previous studies, it is recognized that water co-feeding can inhibit secondary reaction of alkenes by competitively adsorbing on BASs, thus enhancing the alkenes' selectivity and extending the catalytic lifetime.[21−23] The extremely high selectivity of alkanes (ethane and propane, about 60%) in the early reaction stage was attributed to the severe secondary reactions of alkenes in the high-pressure MTO reaction, which is well consistent with previous results.[28] Meanwhile, unlike the increase in alkene selectivity observed in atmospheric-pressure MTO reaction with water co-feeding,[21−23] the selectivity of ethene and propene slightly decreased with increasing water partial pressure from 0.13 MPa to 2.5 MPa (Figures 1(b) and 1(c)). These results indicated that the water presents little effect on inhibiting secondary reaction of alkenes under the high-pressure and high-temperature MTO reaction condition. As observed by

https://doi.org/10.1021/acscatal.4c06239
ACS Catal. 2025, 15, 1553−1562

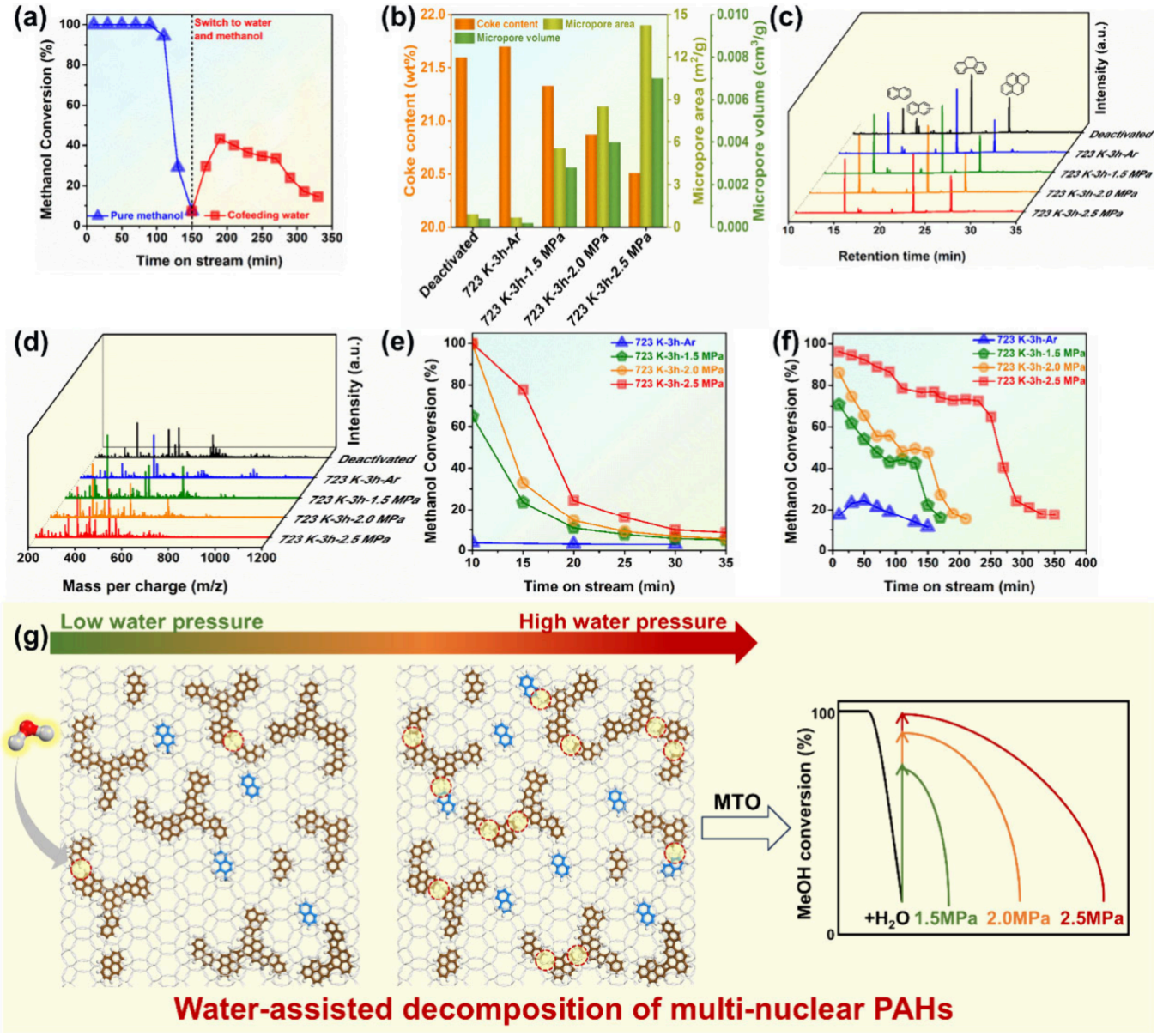

Figure 3. Coke decomposition by high-pressure water under a practical reaction temperature. (a) The reactivity of the deactivated SAPO-34 catalyst upon switching the feed from methanol to water−methanol co-feed with a water partial pressure of 2.5 MPa. (b) The textual property and coke content of the deactivated SAPO-34 catalyst after high-pressure steam treatment. The retained coke species of the deactivated catalyst after steam treatment was detected by GC-MS (c) and MALDI FT-ICR MS (d). The MTO reactivity (pure methanol feeding (e) and methanol−water co-feeding with a water partial pressure of 2.5 MPa (f)) of the steam-treated deactivated catalyst. (g) The molecule model of water-assisted decomposition of multinuclear PAHs over the deactivated catalyst and the recovery of methanol conversion under high-pressure water. Reaction conditions: 723 K, P_{total} = 4.0 MPa, P_{MeOH} = 0.13 MPa, methanol WHSV = 1.0 h^{-1}.

Qian et al. in the ethene aromatization reaction catalyzed by HZSM-5 zeolite, the co-feed water lost its competitive adsorption advantage at temperatures above 623 K.[33] Therefore, although there exists severe hydrogen transfer reaction during the initial reaction stages, the observed significant extension of MTO catalytic lifetime under the high-pressure water co-feeding condition suggests that water may play a crucial role in delaying coking and varying coke species formation and distribution. In addition, the special dynamic catalytic mechanism of the zeolite-catalyzed MTO reaction and the resulting cross-talk effects between diffusion and reaction occurring at multiple scales need to be considered.[34] Thus, a more detailed molecular-level understanding is crucial for elucidating the mechanism of water-delayed coking in a high-pressure MTO reaction.

Molecular Insights into Water-Suppressed PAH Formation within a CHA Cage and Cross-Linking of PAHs between CHA Cages. The retained species on SAPO-34 during the MTO reaction have been extensively studied in previous reports. Structural analyses revealed that there are primarily two types: one includes phenyl, naphthyl, phenanthryl, and pyrenyl species that can be accommodated within a CHA cage, while the other consists of multinuclear structural PAHs formed through the cross-linking of polyaromatics between CHA cages.[26,35] Therefore, we first performed qualitative and quantitative analyses of the retained species on SAPO-34 catalyst after 2 h of methanol conversion

https://doi.org/10.1021/acscatal.4c06239
ACS Catal. 2025, 15, 1553−1562

at different water partial pressures. As shown in Figure 2(a), the total carbonaceous content decreased from 21.4 wt % to 16.0 wt % as the water partial pressure increased from 0.13 MPa to 2.5 MPa, indicating that water effectively suppressed the coke deposition on SAPO-34. It is noteworthy that active hydrocarbon pool species (HCPs) such as phenyl and naphthyl species, which are also retained within the CHA cages due to the restrictions of the eight-membered-ring pores, are included in the measurements. Thus, strictly speaking, the detected species are not exclusively inert carbonaceous species (phenanthryl, pyrenyl, and multinuclear structural PAHs species), and further classification of these species is required. The soluble coke species were detected by GC-MS and shown in Figure 2(b). The CCl_4-soluble fractions obtained from all samples were quite similar, primarily consisting of phenyl, naphthyl, phenanthrene, and pyrene species. This similarity indicates that the co-feeding of water during the high-pressure MTO reaction does not significantly alter the fundamental evolution pathways of the cage-confined aromatic species and, consequently, the associated deactivation mechanisms. Interestingly, the proportions of these cage-confined aromatics among total coke deposits were significantly affected by the water partial pressure (Figure 2(c)). With the water partial pressure increasing from 0.13 MPa to 2.5 MPa, the proportions of phenanthrene and pyrene decreased from 11.8 and 10.3 wt % to 2.7 and 1.9 wt %, respectively, while the proportions of phenyl and naphthyl species increased from 1.6 and 13.0 wt % to 6.0 and 24.8 wt %, respectively. The previous researches indicated that the phenyl and naphthyl species are active HCPs that facilitate the efficient methanol conversion,[27,36−39] but they also act as coke precursors to form the inert phenanthrene and pyrene.[40,41] More specifically, the naphthyl species can undergo a series of reaction such as hydride transfer and deprotonation to form phenanthrene, which can further transform into pyrene through similar pathways.[40,41] Therefore, the significant increase in naphthyl species and the concurrent decrease in phenanthrene and pyrene species under higher water partial pressure suggest that water inhibits the growth of PAHs from ring-fusing of naphthyl species within the CHA cages, thereby maintaining prolonged efficient methanol conversion. Moreover, the growth of multinuclear PAHs is also effectively suppressed under higher water partial pressure, as evidenced by the MALDI FT-ICR MS. As shown in Figure 2(d), the fragment ion groups in m/z ranges of 320−400, 500−600, 680−780, 860−940 Da, etc., are attributed to the multinuclear PAHs via cage-passing growth as identified in our previous studies.[26,35] With the increase of water partial pressure, the decreased signals of multinuclear PAHs demonstrate a suppressed growth of cross-linking PAHs between CHA cages. This inhibition of the cross-cage bonding is primarily due to the strongly suppressed multinuclear PAH precursors, such as phenanthrene and pyrene, within the CHA cages by high-pressure water co-feeding. Additionally, this suppression is intrinsically controlled to some extent by the in situ coke decomposition capability of water under the experimental conditions of high temperature and elevated water partial pressure, which will be discussed in detail in the next section. This suppression is further supported by the thermogravimetric analysis (TGA) (Figure 2(e)), showing that the maximum temperature of differential curves ($T_{G,max}$, the $T_{G,max}$ can reflect the H-unsaturation of coke, i.e., the lower the $T_{G,max}$, the higher the H/C ratio of coke[25,26,42]) decreased from 904 K to 874 K with the water partial pressure increasing from 0.13 MPa to 2.5 MPa. Moreover, UV−vis spectroscopy (Figure 2(f)) revealed that as the water partial pressure increased, the broad absorption peak at ∼550 and ∼630 nm related to the phenanthrene and pyrene species[43−45] decreased markedly with the increase of water partial pressure. In contrast, the signal at ∼270 nm and ∼390 nm attributed to neutral (methylated) benzenes and benzene cation,[46,47] and the signal at 415−450 nm and ∼470 nm assigned to naphthalene and its carbocation species[43−45] showed no obvious changes. These results provide additional spectroscopic evidence that the transformation of naphthyl species to condensed PAHs is effectively inhibited in high-pressure water co-feeding MTO reaction over SAPO-34 catalyst. Figure 2(g) presents a molecular model of water-controlled coke growth under the high-pressure MTO reaction based on the above spectroscopic observations. It is suggested that the co-feeding of water in high-pressure MTO reaction not only controls the growth of aromatics within the CHA cages, particularly the transformation of naphthyl into phenanthrene and pyrene, but also inhibits the cross-linking of PAHs between CHA cages, thereby delaying the coking process of SAPO-34 zeolite catalyst in MTO reaction.

Water-Assisted in Situ Decomposition of Coke Species. At elevated temperatures of 923−953 K, our laboratory has developed a novel regeneration approach wherein steam-assisted cleavage converts inert coke species on SAPO-34 catalyst into naphthyl species which can work as HCPs for MTO reaction.[24−26] Inspired by this development, we sought to determine whether high-pressure steam could facilitate in situ decomposition of coke species under practical MTO reaction conditions of 723 K. To address this, we have designed a series of experiments focusing on water switching and steam-assisted cleavage and conducted detailed investigations into coke species evolution. As shown in Figure 3(a), after methanol conversion for 150 min with the occurrence of catalyst deactivation, upon switching the feed from methanol to water−methanol co-feed with a water partial pressure of 2.5 MPa, the methanol conversion gradually recovered from 5% to 43%. This result preliminarily suggests that the coke species blocking or covering the active sites were partially decomposed by water to realize the activation of the catalyst to some extent, leading to a partial restoration of the MTO catalytic activity of SAPO-34. Further investigation involves steam treatment of the deactivated SAPO-34 catalyst at the actual MTO reaction temperature (723 K) under varying water partial pressures (1.5−2.5 MPa). As shown in Figure 3(b), a slight reduction in coke content from 21.6 to 20.4 wt % and concurrent increase in the accessible porosity/cavity (micropore volume and micropore surface area measurable by the N_2-adsorption technique) can be observed over the samples after steam treatment. Meanwhile, the results of NH_3-TPD showed that the active acidic sites were also partially recovered (Figure S3). These findings demonstrated that under MTO reaction conditions high-pressure steam can partially decompose the coke species on SAPO-34 in situ, with this decomposition ability positively correlated with water partial pressure. This observation aligns with the extended catalytic lifetime of SAPO-34 under water co-feeding with higher partial pressure, as shown in Figure 1(a).

Furthermore, coke species confined in SAPO-34 after steam treatment under 723 K were detected by GC-MS and MALDI FT-ICR MS, as shown in Figures 3(c) and 3(d). GC-MS analysis revealed a significant reduction in the number of

https://doi.org/10.1021/acscatal.4c06239
ACS Catal. 2025, 15, 1553−1562

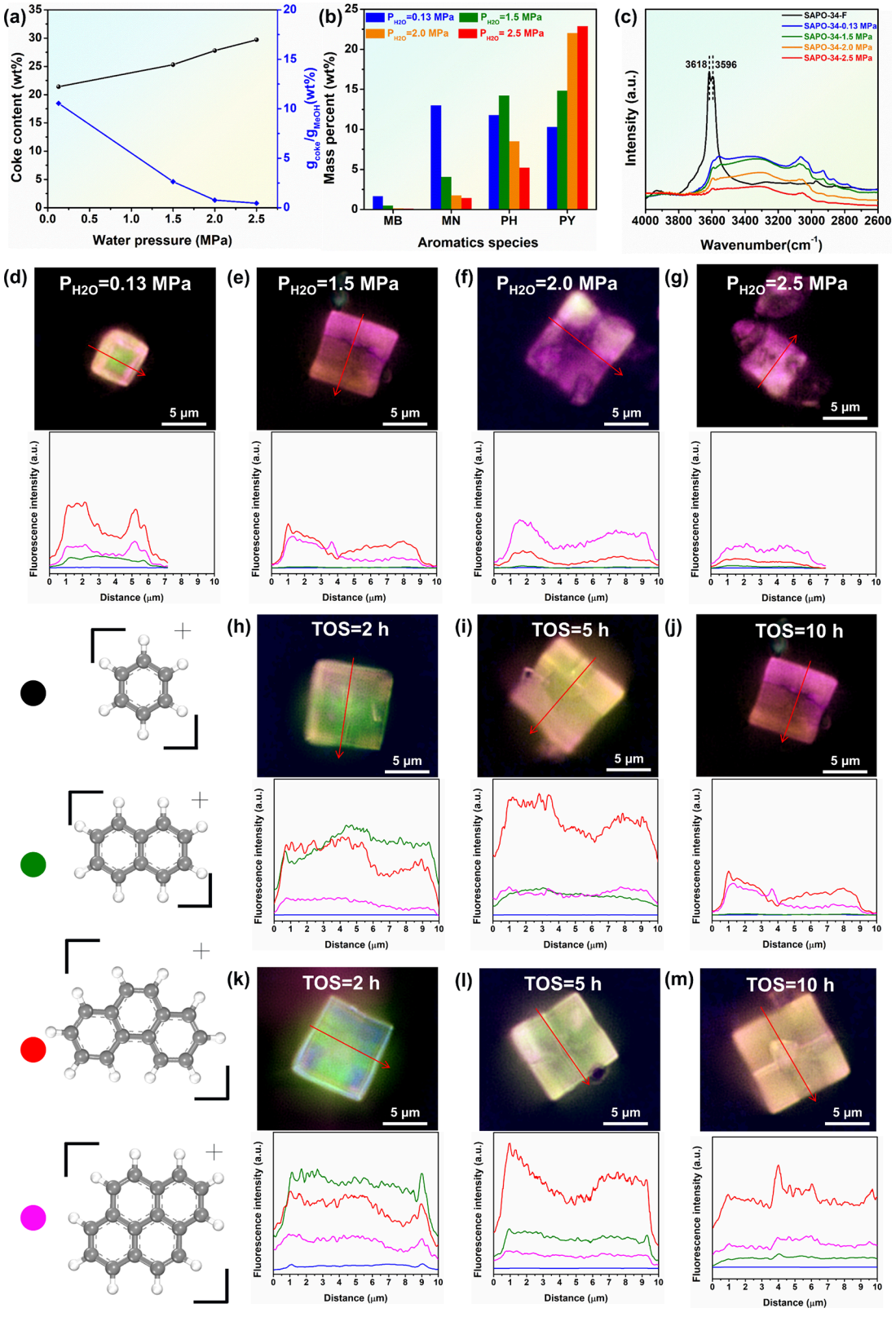

Figure 4. Visualization of water-controlled coking dynamics and the improvement in diffusion efficiency with different water partial pressures. (a) The total coke content of deactivated catalysts. (b) Detailed distribution of CCl_4-soluble fractions of the retained organics extracted among total coke over the deactivated catalysts. (c) The FTIR spectra of deactivated catalysts. The spatiotemporal distribution and fluorescence intensities of aromatic species obtained from SIM on deactivated SAPO-34 catalyst are 0.13 MPa (d), 1.5 MPa (e), 2.0 MPa (f), and 2.5 MPa (g). The distribution and fluorescence intensities of aromatic species in the MTO dynamic evolution process with water partial pressures of 1.5 MPa (h−j) and 2.5 MPa (k−m). Reaction conditions: 723 K, P_{total} = 4.0 MPa, P_{MeOH} = 0.13 MPa methanol, WHSV = 1.0 h^{-1}.

https://doi.org/10.1021/acscatal.4c06239
ACS Catal. 2025, 15, 1553−1562

aromatic species with alkyl side chains (Figure 3(c)). Specifically, the naphthyl species exhibited significant signal changes, with alkyl-substituted naphthalenes decreasing and naphthalene increasing after steam treatment. These results suggest that high-pressure water has promoted the degradation of soluble aromatic species within the CHA cages, primarily reflected in the elimination of alkyl side chains from the aromatics, which has been proved by our recent work.[26] As steam pressure was increased, a significant attenuation around the 900 Da signal in the MALDI FT-ICR MS spectroscopy was observed, indicating the impact of steam treatment on coke species (Figure 3(d)). This decrease is likely due to the hydrolytic action of water molecules at the cross-cage junctions, which disrupts the compact structure of the multinuclear PAHs. At 723 K, although steam treatment does not completely remove these multinuclear PAH coke species, the shearing effect of water molecules induces a structural transition from dense PAHs to dispersed aromatics accommodation. This transition undoubtedly facilitates the diffusion and transport of water and reactant molecules within the SAPO-34 zeolite matrix. The differential TG curves showed a decrease in the maximum temperature ($T_{G,\,max}$) from 907 K to 899 K (Figure S4), and the color of the CCl_4 organic extract (solution lower layer) gradually changed from brown to light yellow during HF solution dissolution (Figure S5), further indicating the cleavage of highly H-unsaturated coke species by high-pressure steam. Consequently, at the reaction temperature of 723 K, the deactivation trend of SAPO-34 catalyst can be partially neutralized or reversed, confirming the in situ coke decomposition capability of high-pressure water during the MTO reaction.

Water partial pressure is a pivotal factor in water-assisted deactivated catalyst regeneration. The recovery of methanol conversion on regenerated SAPO-34 has been investigated after steam treatment at various pressures, as depicted in Figure 3(e). The methanol conversion can be recovered from 5% to 100% on the deactivated SAPO-34 catalyst after steam treatment at water partial pressures of 2.0 and 2.5 MPa, while those treated at 1.5 MPa recovered only to 65%. In contrast, the argon-treated sample showed no significant change compared to the pretreatment levels. The restoration of methanol conversion substantiates the in situ coke decomposition capability of high-pressure water in the MTO reaction, yet it is insufficient to counteract the growth trend of coke species. In the absence of high-pressure water, pure methanol feed leads to the rapid re-establishment of PAHs within and/or between the CHA cages of SAPO-34, resulting in swift re-deactivation. Compared to pure methanol feeding, the water−methanol co-feeding onto the steam-treated SAPO-34 catalyst exhibited a reduced rate of coke deposition and an extended catalytic lifetime (Figure 3(f)), which further supports the inhibitory effect of high-pressure water on coke formation and growth. Figure 3(g) exhibits the molecular model of water-assisted decomposition of multinuclear PAHs over the deactivated catalyst and the recovery of methanol conversion under the high-pressure MTO reaction based on the above spectroscopic results. It is noteworthy that the coke decomposition capability increases with the water partial pressure at the real MTO reaction temperature, as well as the more significant recovery of methanol conversion, thereby offering both parametric and theoretical support for the steam-assisted regeneration strategy for the reaction-regeneration technology of the MTO process.

Visualization of Water-Controlled Coking Dynamics and the Improvement in Diffusion Efficiency. SAPO-34 molecular sieve drives efficient methanol conversion through the confinement of aromatic species within CHA cages, and these confined species dynamically evolve with MTO reaction.[48,49] As these aromatic species undergo intensified polycondensation, their occupation or modification of CHA cages will inevitably lead to severe diffusion and transport limitations for reactant and product molecules.[32,34,50] Therefore, these confined aromatics and their evolution are crucial for the diffusion of methanol and light olefins within the SAPO-34 crystallites.

As shown in Figure 4(a), the coke content of the deactivated catalysts (the catalysts with methanol conversion dropping to about 80%) significantly increased from 21.4 to 29.7 wt % with the water partial pressure increasing from 0.13 to 2.5 MPa, suggesting that more coke species are accommodated on the deactivated SAPO-34 catalyst under the high-pressure water co-feeding MTO reaction. In addition, the ratio of methanol consumption on coke formation decreased from 10.5 to 0.45 wt % with the water partial pressure increasing from 0.13 to 2.5 MPa (Figure 4(a)). This result demonstrates that the high-pressure water suppresses the transformation of methanol feed to coke deposition, which is consistent with the above-mentioned results of high-pressure water inhibiting the coke deposition formation, thus extending the catalytic lifetime. GC-MS analysis of soluble coke species on the deactivated SAPO-34 catalyst (Figures 4(b) and S6) showed that as the water partial pressure increased from 0.13 to 2.5 MPa, the proportions of phenyl and naphthyl species in the total coke gradually decreased from 1.6 and 13.0 wt % to 0.1 and 1.4 wt %, respectively, while the proportion of pyrene significantly increased from 10.3 to 22.8 wt %. This is consistent with the observed higher proportion of insoluble substances during HF solution dissolution (Figure S7, the insoluble and black substances gradually appearing and increasing in the upper layer) and the higher $T_{G,max}$ detected by the TGA (Figure S8, the $T_{G,max}$ increased from 904 to 948 K) over the deactivated SAPO-34 catalyst with the increase of water partial pressure. An FTIR spectrometer was employed to detect the unoccupied or unused bridging hydroxyl groups on the deactivated SAPO-34 catalyst. Due to the consumption or occupation of bridging hydroxyl groups, there is a pronounced reduction in the intensity of the absorbance at both 3618 and 3596 cm^{-1} (characteristic peak for bridging hydroxyl groups[51,52]) with the water partial pressure increase (Figure 4(c)). Normalized to the signal intensity obtained from the fresh SAPO-34 catalyst, the utilization factor of BASs increased from 75% to 95% as the water partial pressure increased from 0.13 to 2.5 MPa. Therefore, these results preliminarily indicate that the water co-feeding in high-pressure MTO reaction ultimately enhances the utilization efficiency of BASs within SAPO-34 catalyst, allowing more coke species to be accommodated within a single crystal.

More intuitively, advanced super-resolution structured illumination microscopy (SIM) was conducted to visualize the spatiotemporal distribution of coke species within individual SAPO-34 crystals during the MTO reaction with different water partial pressures. The previous studies confirmed that characteristic UV−vis adsorption bands of benzene-, naphthalene-, phenanthrene- and pyrene-based carbenium ions were around 390, 480, 560, and 640 nm, respectively, with corresponding emission wavelengths in the

https://doi.org/10.1021/acscatal.4c06239
ACS Catal. 2025, 15, 1553−1562

ranges of 480−490, 500−520, 620−630, and 670−700 nm.[43−45,50,53] At a low water partial pressure of 0.13 MPa, the constrained species were concentrated in the crystal rim, predominantly phenanthrene and pyrene (Figure 4(d)). These inert polyaromatics occupied and blocked the CHA cages at the crystal edges, inhibiting the diffusion of methanol into the inner core regions, leading to rapid catalyst deactivation. As observed in the FTIR (Figure 4(c)), significant BASs remain unutilized under low water partial pressure conditions. However, as the water partial pressure increased to 1.5, 2.0, and 2.5 MPa (Figures 4(e−g)), the coke species gradually extended from the crystal edges toward the core regions. Particularly at 2.5 MPa, a relatively uniform distribution throughout the whole SAPO-34 crystal suggests that the crystal space and/or acidic sites were almost fully utilized, indicating the accommodation of more coke deposits. More specifically, the dynamic evolution of coke growth and distribution during the MTO reaction at water partial pressures of 1.5 and 2.5 MPa was monitored using SIM, as shown in Figures 4(h−j) and 4(k−m), respectively. For the visualization at a water partial pressure of 1.5 MPa, naphthyl species were distributed over the greatest area of SAPO-34 crystals and the fluorescence intensity gradually decreased, while the intensity of phenanthrene and pyrene increased with time on stream (TOS) from 2 h to 5 h and to 10 h, indicating the accumulation of the inert coke species. For the visualization at a water partial pressure of 2.5 MPa, a more uniform distribution of naphthyl species can be observed during the TOS from 2 to 5 h and gradually transformed to phenanthrene at the TOS of 10 h. Through the observation by SIM, we have gained direct insights into the coking dynamics and spatial structural evolution of coke species within individual SAPO-34 crystals during MTO reaction under high-pressure water co-feeding conditions. Water controls the growth and cross-linking of coke within and between the CHA cages, improving the diffusion and transport of methanol and hydrocarbon products within the SAPO-34 crystals. The cross-talk of water-controlled coking and diffusion dynamics enhances the utilization efficiency of BASs and micropores within SAPO-34 crystals, resulting in a more uniform coke distribution and an extended catalytic lifetime of the MTO reaction.

CONCLUSION

In summary, our study elucidates the critical role of water as a co-feed and decoking agent in high-pressure MTO reaction over SAPO-34 zeolite catalyst. Through a suite of analytical techniques, we have demonstrated that water significantly influences the coking dynamics and diffusion efficiency within SAPO-34. Specifically, co-feeding high-pressure water suppresses the polycyclization of active HCPs within the CHA cages and hinders the cross-linking of PAHs between CHA cages. In situ water-switching and steam treatment experiments further validate the capability of water to decompose coke species under real MTO reaction conditions, with methanol conversion rates recovering significantly upon water co-feeding and high-pressure steam treatment. These improve the diffusion and transport of reactants and products into the inner core regions of SAPO-34 crystals, resulting in a more uniform coke distribution and enhancing the utilization of active sites within the micropores. The water-controlled coke growth, water-assisted in situ decomposition of coke species, and water-promoted utilization efficiency of SAPO-34 crystals together enhance the catalytic performance and extend the catalytic lifetime of the SAPO-34 catalyst. The mechanistic insights gained from this study provide a crucial theoretical foundation for the application of water-related techniques in the MTO industrial processes. These findings underscore the potential of integrating water co-feeding and steam-assisted regeneration strategies to optimize MTO catalysis, ultimately contributing to more efficient and sustainable industrial practices.

ASSOCIATED CONTENT

Supporting Information

The Supporting Information is available free of charge at https://pubs.acs.org/doi/10.1021/acscatal.4c06239.

Materials and characterization, experimental details, catalyst characterization results, and additional data and figures (PDF)

AUTHOR INFORMATION

Corresponding Authors

Yingxu Wei − *National Engineering Research Center of Lower-Carbon Catalysis Technology, Dalian National Laboratory for Clean Energy, iChEM (Collaborative Innovation Center of Chemistry for Energy Materials), Dalian Institute of Chemical Physics, Chinese Academy of Sciences, Dalian 116023, China;* orcid.org/0000-0002-0412-1980; Email: weiyx@dicp.ac.cn

Xinqiang Wu − *National Engineering Research Center of Lower-Carbon Catalysis Technology, Dalian National Laboratory for Clean Energy, iChEM (Collaborative Innovation Center of Chemistry for Energy Materials), Dalian Institute of Chemical Physics, Chinese Academy of Sciences, Dalian 116023, China*; Email: wuxinqiang@dicp.ac.cn

Authors

Chengwei Zhang − *National Engineering Research Center of Lower-Carbon Catalysis Technology, Dalian National Laboratory for Clean Energy, iChEM (Collaborative Innovation Center of Chemistry for Energy Materials), Dalian Institute of Chemical Physics, Chinese Academy of Sciences, Dalian 116023, China; University of Chinese Academy of Sciences, Beijing 100049, China*

Yanan Zhang − *National Engineering Research Center of Lower-Carbon Catalysis Technology, Dalian National Laboratory for Clean Energy, iChEM (Collaborative Innovation Center of Chemistry for Energy Materials), Dalian Institute of Chemical Physics, Chinese Academy of Sciences, Dalian 116023, China; University of Chinese Academy of Sciences, Beijing 100049, China*

Li Wang − *Division of Energy Research Resources, CAS Key Laboratory of Separation Science for Analytical Chemistry, Dalian Institute of Chemical Physics, Chinese Academy of Sciences, Dalian 116023, China*

Yan Jin − *Division of Energy Research Resources, CAS Key Laboratory of Separation Science for Analytical Chemistry, Dalian Institute of Chemical Physics, Chinese Academy of Sciences, Dalian 116023, China;* orcid.org/0000-0002-3694-9723

Mingbin Gao − *State Key Laboratory of Physical Chemistry of Solid Surfaces, College of Chemistry and Chemical Engineering, Xiamen University, Xiamen 361005, China*

https://doi.org/10.1021/acscatal.4c06239
ACS Catal. 2025, 15, 1553−1562

Mao Ye − *National Engineering Research Center of Lower-Carbon Catalysis Technology, Dalian National Laboratory for Clean Energy, iChEM (Collaborative Innovation Center of Chemistry for Energy Materials), Dalian Institute of Chemical Physics, Chinese Academy of Sciences, Dalian 116023, China;* orcid.org/0000-0002-7078-2402

Zhongmin Liu − *National Engineering Research Center of Lower-Carbon Catalysis Technology, Dalian National Laboratory for Clean Energy, iChEM (Collaborative Innovation Center of Chemistry for Energy Materials), Dalian Institute of Chemical Physics, Chinese Academy of Sciences, Dalian 116023, China; State Key Laboratory of Catalysis, Dalian Institute of Chemical Physics, Chinese Academy of Sciences, Dalian 116023, China; University of Chinese Academy of Sciences, Beijing 100049, China;* orcid.org/0000-0002-7999-2940

Complete contact information is available at: https://pubs.acs.org/10.1021/acscatal.4c06239

Notes

The authors declare no competing financial interest.

■ ACKNOWLEDGMENTS

The authors are thankful for the financial support from the National Key R&D Program of China (Grant No. 2021YFA1502600), the National Natural Science Foundation of China (Grant Nos. 22372163, 21902153, 22288101, 21991092, 21991090), and the Youth Innovation Promotion Association, CAS (Grant No. 2022182). The authors also thank Hanlixin Wang, Dr. Qinglong Qiao, and Prof. Zhaochao Xu at Dalian Institute of Chemical Physics, Chinese Academy of Sciences, for the help in SIM imaging.

■ REFERENCES

(1) Wu, Z.; Chen, J.; Wang, Y.; Zhu, Y.; Liu, Y.; Yao, B.; Zhang, Y.; Hu, M. Interactions between Water Vapor and Atmospheric Aerosols Have Key Roles in Air Quality and Climate Change. *Natl. Sci. Rev.* **2018**, *5*, 452−454.

(2) Ball, P. Water — an Enduring Mystery. *Nature.* **2008**, *452*, 291−292.

(3) Hu, J.; Cao, Z. Water Science on the Molecular Scale: New Insights into the Characteristics of Water. *Natl. Sci. Rev.* **2014**, *1*, 179−181.

(4) Shi, J.; Wang, Y.; Yang, W.; Tang, Y.; Xie, Z. Recent Advances of Pore System Construction in Zeolite-Catalyzed Chemical Industry Processes. *Chem. Soc. Rev.* **2015**, *44*, 8877−8903.

(5) Pérez-Botella, E.; Valencia, S.; Rey, F. Zeolites in Adsorption Processes: State of the Art and Future Prospects. *Chem. Rev.* **2022**, *122*, 17647−17695.

(6) Yue, B.; Liu, S.; Chai, Y.; Wu, G.; Guan, N.; Li, L. Zeolites for Separation: Fundamental and Application. *J. Energy Chem.* **2022**, *71*, 288−303.

(7) Cooper, E. R.; Andrews, C. D.; Wheatley, P. S.; Webb, P. B.; Wormald, P.; Morris, R. E. Ionic Liquids and Eutectic Mixtures as Solvent and Template in Synthesis of Zeolite Analogues. *Nature.* **2004**, *430*, 1012−1016.

(8) Ma, H.; Tian, Z.; Xu, R.; Wang, B.; Wei, Y.; Wang, L.; Xu, Y.; Zhang, W.; Lin, L. Effect of Water on the Ionothermal Synthesis of Molecular Sieves. *J. Am. Chem. Soc.* **2008**, *130*, 8120−8121.

(9) Kasneryk, V.; Shamzhy, M.; Zhou, J.; Yue, Q.; Mazur, M.; Mayoral, A.; Luo, Z.; Morris, R. E.; Cejka, J.; Opanasenko, M. Vapour-Phase-Transport Rearrangement Technique for the Synthesis of New Zeolites. *Nat. Commun.* **2019**, *10*, 5129.

(10) Prodinger, S.; Derewinski, M. A.; Vjunov, A.; Burton, S. D.; Arslan, I.; Lercher, J. A. Improving Stability of Zeolites in Aqueous Phase Via Selective Removal of Structural Defects. *J. Am. Chem. Soc.* **2016**, *138*, 4408−15.

(11) Heard, C. J.; Grajciar, L.; Uhlik, F.; Shamzhy, M.; Opanasenko, M.; Cejka, J.; Nachtigall, P. Zeolite (in)Stability under Aqueous or Steaming Conditions. *Adv. Mater.* **2020**, *32*, No. e2003264.

(12) Minova, I. B.; Barrow, N. S.; Sauerwein, A. C.; Naden, A. B.; Cordes, D. B.; Slawin, A. M. Z.; Schuyten, S. J.; Wright, P. A. Silicon Redistribution, Acid Site Loss and the Formation of a Core−Shell Texture Upon Steaming Sapo-34 and Their Impact on Catalytic Performance in the Methanol-to-Olefins (MTO) Reaction. *J. Catal.* **2021**, *395*, 425−444.

(13) Stanciakova, K.; Weckhuysen, B. M. Water−Active Site Interactions in Zeolites and Their Relevance in Catalysis. *Trends Chem.* **2021**, *3*, 456−468.

(14) Liu, Q.; van Bokhoven, J. A. Water Structures on Acidic Zeolites and Their Roles in Catalysis. *Chem. Soc. Rev.* **2024**, *53*, 3065−3095.

(15) Olsbye, U.; Svelle, S.; Lillerud, K. P.; Wei, Z. H.; Chen, Y. Y.; Li, J. F.; Wang, J. G.; Fan, W. B. The Formation and Degradation of Active Species During Methanol Conversion over Protonated Zeotype Catalysts. *Chem. Soc. Rev.* **2015**, *44*, 7155−76.

(16) Tian, P.; Wei, Y.; Ye, M.; Liu, Z. Methanol to Olefins (MTO): From Fundamentals to Commercialization. *ACS Catal.* **2015**, *5*, 1922−1938.

(17) Yarulina, I.; Chowdhury, A. D.; Meirer, F.; Weckhuysen, B. M.; Gascon, J. Recent Trends and Fundamental Insights in the Methanol-to-Hydrocarbons Process. *Nat. Catal.* **2018**, *1*, 398−411.

(18) Wang, S.; Qin, Z.; Dong, M.; Wang, J.; Fan, W. Recent Progress on MTO Reaction Mechanisms and Regulation of Acid Site Distribution in the Zeolite Framework. *Chem. Catalysis.* **2022**, *2*, 1657−1685.

(19) Yang, M.; Fan, D.; Wei, Y.; Tian, P.; Liu, Z. Recent Progress in Methanol-to-Olefins (MTO) Catalysts. *Adv. Mater.* **2019**, *31*, 1902181.

(20) Sun, Q.; Xie, Z.; Yu, J. The State-of-the-Art Synthetic Strategies for SAPO-34 Zeolite Catalysts in Methanol-to-Olefin Conversion. *Natl. Sci. Rev.* **2018**, *5*, 542−558.

(21) Marchi, A. J.; Froment, G. F. Catalytic Conversion of Methanol to Light Alkenes on SAPO Molecular Sieves. *Appl. Catal.* **1991**, *71*, 139−152.

(22) Wu, X.; Anthony, R. G. Effect of Feed Composition on Methanol Conversion to Light Olefins over SAPO-34. *Appl. Catal. A-Gen.* **2001**, *218*, 241−250.

(23) De Wispelaere, K.; Wondergem, C. S.; Ensing, B.; Hemelsoet, K.; Meijer, E. J.; Weckhuysen, B. M.; Van Speybroeck, V.; Ruiz-Martínez, J. Insight into the Effect of Water on the Methanol-to-Olefins Conversion in H-SAPO-34 from Molecular Simulations and in Situ Microspectroscopy. *ACS Catal.* **2016**, *6*, 1991−2002.

(24) Zhou, J.; Zhang, J.; Zhi, Y.; Zhao, J.; Zhang, T.; Ye, M.; Liu, Z. Partial Regeneration of the Spent SAPO-34 Catalyst in the Methanol-to-Olefins Process Via Steam Gasification. *Ind. Eng. Chem. Res.* **2018**, *57*, 17338−17347.

(25) Zhou, J.; Gao, M.; Zhang, J.; Liu, W.; Zhang, T.; Li, H.; Xu, Z.; Ye, M.; Liu, Z. Directed Transforming of Coke to Active Intermediates in Methanol-to-Olefins Catalyst to Boost Light Olefins Selectivity. *Nat. Commun.* **2021**, *12*, 17.

(26) Wang, N.; Wang, L.; Zhi, Y.; Han, J.; Zhang, C.; Wu, X.; Zhang, J.; Wang, L.; Fan, B.; Xu, S.; Zheng, Y.; Lin, S.; Wu, R.; Wei, Y.; Liu, Z. Coking and Decoking Chemistry for Resource Utilization of Polycyclic Aromatic Hydrocarbons (PAHs) and Low-Carbon Process. *J. Energy Chem.* **2023**, *76*, 105−116.

(27) Zhang, C.; Wu, X.; Zhang, Y.; Zhang, W.; Lin, S.; Lou, C.; Xu, S.; He, D.; Wang, L.; Wei, Y.; Liu, Z. Water-Assisted Shape-Selective Production of Ethene in Methanol-to-Olefins Reaction on SAPO-34. *Chem. Catalysis.* **2024**, *4*, 101025.

(28) Zhao, X.; Li, J.; Tian, P.; Wang, L.; Li, X.; Lin, S.; Guo, X.; Liu, Z. Achieving a Superlong Lifetime in the Zeolite-Catalyzed MTO Reaction under High Pressure: Synergistic Effect of Hydrogen and Water. *ACS Catal.* **2019**, *9*, 3017−3025.

(29) Arora, S. S.; Nieskens, D. L. S.; Malek, A.; Bhan, A. Lifetime Improvement in Methanol-to-Olefins Catalysis over Chabazite Materials by High-Pressure H_2 Co-Feeds. *Nat. Catal.* **2018**, *1*, 666−672.
(30) Mores, D.; Stavitski, E.; Kox, M. H.; Kornatowski, J.; Olsbye, U.; Weckhuysen, B. M. Space- and Time-Resolved in-Situ Spectroscopy on the Coke Formation in Molecular Sieves: Methanol-to-Olefin Conversion over H-ZSM-5 and H-SAPO-34. *Chemistry.* **2008**, *14*, 11320−7.
(31) Dai, W.; Scheibe, M.; Li, L.; Guan, N.; Hunger, M. Effect of the Methanol-to-Olefin Conversion on the PFG NMR Self-Diffusivities of Ethane and Ethene in Large-Crystalline Sapo-34. *J. Phys. Chem. C* **2012**, *116*, 2469−2476.
(32) Gao, S.; Xu, S.; Wei, Y.; Qiao, Q.; Xu, Z.; Wu, X.; Zhang, M.; He, Y.; Xu, S.; Liu, Z. Insight into the Deactivation Mode of Methanol-to-Olefins Conversion over SAPO-34: Coke, Diffusion, and Acidic Site Accessibility. *J. Catal.* **2018**, *367*, 306−314.
(33) Wang, H.; Hou, Y.; Sun, W.; Hu, Q.; Xiong, H.; Wang, T.; Yan, B.; Qian, W. Insight into the Effects of Water on the Ethene to Aromatics Reaction with HZSM-5. *ACS Catal.* **2020**, *10*, 5288−5298.
(34) Lin, S.; Zhi, Y.; Liu, Z.; Yuan, J.; Liu, W.; Zhang, W.; Xu, Z.; Zheng, A.; Wei, Y.; Liu, Z. Multiscale Dynamical Cross-Talk in Zeolite-Catalyzed Methanol and Dimethyl Ether Conversions. *Natl. Sci. Rev.* **2022**, *9*, No. nwac151.
(35) Wang, N.; Zhi, Y.; Wei, Y.; Zhang, W.; Liu, Z.; Huang, J.; Sun, T.; Xu, S.; Lin, S.; He, Y.; Zheng, A.; Liu, Z. Molecular Elucidating of an Unusual Growth Mechanism for Polycyclic Aromatic Hydrocarbons in Confined Space. *Nat. Commun.* **2020**, *11*, 1079.
(36) Li, J.; Wei, Y.; Chen, J.; Tian, P.; Su, X.; Xu, S.; Qi, Y.; Wang, Q.; Zhou, Y.; He, Y.; Liu, Z. Observation of Heptamethylbenzenium Cation over Sapo-Type Molecular Sieve DNL-6 under Real MTO Conversion Conditions. *J. Am. Chem. Soc.* **2012**, *134*, 836−9.
(37) Xu, S.; Zheng, A.; Wei, Y.; Chen, J.; Li, J.; Chu, Y.; Zhang, M.; Wang, Q.; Zhou, Y.; Wang, J.; Deng, F.; Liu, Z. Direct Observation of Cyclic Carbenium Ions and Their Role in the Catalytic Cycle of the Methanol-to-Olefin Reaction over Chabazite Zeolites. *Angew. Chem., Int. Ed.* **2013**, *52*, 11564−8.
(38) Zhang, W.; Chen, J.; Xu, S.; Chu, Y.; Wei, Y.; Zhi, Y.; Huang, J.; Zheng, A.; Wu, X.; Meng, X.; Xiao, F.; Deng, F.; Liu, Z. Methanol to Olefins Reaction over Cavity-Type Zeolite: Cavity Controls the Critical Intermediates and Product Selectivity. *ACS Catal.* **2018**, *8*, 10950−10963.
(39) Zhou, J.; Zhi, Y.; Zhang, J.; Liu, Z.; Zhang, T.; He, Y.; Zheng, A.; Ye, M.; Wei, Y.; Liu, Z. Presituated "Coke"-Determined Mechanistic Route for Ethene Formation in the Methanol-to-Olefins Process on SAPO-34 Catalyst. *J. Catal.* **2019**, *377*, 153−162.
(40) Wang, S.; Chen, Y.; Wei, Z.; Qin, Z.; Liang, T.; Dong, M.; Li, J.; Fan, W.; Wang, J. Evolution of Aromatic Species in Supercages and Its Effect on the Conversion of Methanol to Olefins over H-MCM-22 Zeolite: A Density Functional Theory Study. *J. Phys. Chem. C* **2016**, *120*, 27964−27979.
(41) Fan, S.; Wang, H.; Wang, P.; Jiao, W.; Wang, S.; Qin, Z.; Dong, M.; Wang, J.; Fan, W. Formation and Evolution of the Coke Precursors on the Zeolite Catalyst in the Conversion of Methanol to Olefins. *Chem. Catalysis.* **2024**, *4*, 100927.
(42) Magnoux, P.; Guisnet, M.; Mignard, S.; Cartraud, P. Coking, Aging, and Regeneration of Zeolites: Viii. Nature of Coke Formed on Hydrogen Offretite During n-Heptane Cracking: Mode of Formation. *J. Catal.* **1989**, *117*, 495−502.
(43) Van Speybroeck, V.; Hemelsoet, K.; De Wispelaere, K.; Qian, Q.; Van der Mynsbrugge, J.; De Sterck, B.; Weckhuysen, B. M.; Waroquier, M. Mechanistic Studies on Chabazite-Type Methanol-to-Olefin Catalysts: Insights from Time-Resolved UV/Vis Microspectroscopy Combined with Theoretical Simulations. *ChemCatChem.* **2013**, *5*, 173−184.
(44) Hemelsoet, K.; Qian, Q.; De Meyer, T.; De Wispelaere, K.; De Sterck, B.; Weckhuysen, B. M.; Waroquier, M.; Van Speybroeck, V. Identification of Intermediates in Zeolite-Catalyzed Reactions by in Situ UV/Vis Microspectroscopy and a Complementary Set of Molecular Simulations. *Chem.—Eur. J.* **2013**, *19*, 16595−606.
(45) Borodina, E.; Meirer, F.; Lezcano-González, I.; Mokhtar, M.; Asiri, A. M.; Al-Thabaiti, S. A.; Basahel, S. N.; Ruiz-Martinez, J.; Weckhuysen, B. M. Influence of the Reaction Temperature on the Nature of the Active and Deactivating Species During Methanol to Olefins Conversion over H-SSZ-13. *ACS Catal.* **2015**, *5*, 992−1003.
(46) Bjørgen, M.; Bonino, F.; Kolboe, S.; Lillerud, K.-P.; Zecchina, A.; Bordiga, S. Spectroscopic Evidence for a Persistent Benzenium Cation in Zeolite H-Beta. *J. Am. Chem. Soc.* **2003**, *125*, 15863−15868.
(47) Dai, W.; Wu, G.; Li, L.; Guan, N.; Hunger, M. Mechanisms of the Deactivation of SAPO-34 Materials with Different Crystal Sizes Applied as Mto Catalysts. *ACS Catal.* **2013**, *3*, 588−596.
(48) Wu, X.; Wei, Y.; Liu, Z. Dynamic Catalytic Mechanism of the Methanol-to-Hydrocarbons Reaction over Zeolites. *Acc. Chem. Res.* **2023**, *56*, 2001−2014.
(49) Zhang, W.; Lin, S.; Wei, Y.; Tian, P.; Ye, M.; Liu, Z. Cavity-Controlled Methanol Conversion over Zeolite Catalysts. *Natl. Sci. Rev.* **2023**, *10*, No. nwad120.
(50) Gao, M.; Li, H.; Liu, W.; Xu, Z.; Peng, S.; Yang, M.; Ye, M.; Liu, Z. Imaging Spatiotemporal Evolution of Molecules and Active Sites in Zeolite Catalyst During Methanol-to-Olefins Reaction. *Nat. Commun.* **2020**, *11*, 3641.
(51) Smith, L.; Cheetham, A. K.; Marchese, L.; Thomas, J. M.; Wright, P. A.; Chen, J.; Gianotti, E. A Quantitative Description of the Active Sites in the Dehydrated Acid Catalyst HAPO-34 for the Conversion of Methanol to Olefins. *Catal. Lett.* **1996**, *41*, 13−16.
(52) Bordiga, S.; Regli, L.; Cocina, D.; Lamberti, C.; Bjørgen, M.; Lillerud, K. P. Assessing the Acidity of High Silica Chabazite H-SSZ-13 by Ftir Using Co as Molecular Probe: Comparison with H-SAPO-34. *J. Phys. Chem. B* **2005**, *109*, 2779−2784.
(53) Qian, Q.; Ruiz-Martinez, J.; Mokhtar, M.; Asiri, A. M.; Al-Thabaiti, S. A.; Basahel, S. N.; van der Bij, H. E.; Kornatowski, J.; Weckhuysen, B. M. Single-Particle Spectroscopy on Large Sapo-34 Crystals at Work: Methanol-to-Olefin Versus Ethanol-to-Olefin Processes. *Chemistry.* **2013**, *19*, 11204−15.

https://doi.org/10.1021/acscatal.4c06239
ACS Catal. 2025, 15, 1553−1562